

Contingency-Aware Planning via Certified Neural Hamilton–Jacobi Reachability

Kasidit Muenprasitvej and Derya Aksaray

Abstract—Hamilton–Jacobi (HJ) reachability provides formal safety guarantees for dynamical systems, but solving high-dimensional HJ partial differential equations limits its use in real-time planning. This paper presents a contingency-aware multi-goal navigation framework that integrates learning-based reachability with sampling-based planning in unknown environments. We use Fourier Neural Operator (FNO) to approximate the solution operator of the Hamilton–Jacobi–Isaacs variational inequality under varying obstacle configurations. We first provide a theoretical under-approximation guarantee on the safe backward reach-avoid set, which enables formal safety certification of the learned reachable sets. Then, we integrate the certified reachable sets with an incremental multi-goal planner, which enforces reachable-set constraints and a recovery policy that guarantees finite-time return to a safe region. Overall, we demonstrate that the proposed framework achieves asymptotically optimal navigation with provable contingency behavior, and validate its performance through real-time deployment on KUKA’s youBot in Webots simulation¹.

I. INTRODUCTION

Ensuring provably safe autonomy while maintaining computational tractability remains a central challenge in robotic planning. Contingency planning addresses this by equipping the system with certified fallback maneuvers that guarantee recovery in the face of adversary events. In this paper, we propose a learning-enabled Hamilton–Jacobi (HJ) reach-avoid framework that ensures a robot always maintains a finite-time recovery path to a safe region during multi-goal navigation in initially unknown environments.

A. Related Work

1) *Contingency Planning and Safety Certificates*: Contingency planning frameworks commonly employ backup behaviors paired with safety certificates. For example, Model Predictive Control (MPC) (e.g., [1]) enforces safety through online constrained optimization, but may suffer infeasibility under tight computational budgets. Control Barrier Functions (CBFs) (e.g., [2]) cast safety enforcement as a quadratic program, though their applicability depends on constructing valid barrier certificates. Precomputed fallback policies (e.g., [3]) switch to predetermined safe behaviors upon contingency detection, though requiring careful design of the switching logic. Hamilton–Jacobi (HJ) reachability [4] provides certified safe sets against worst-case disturbance and

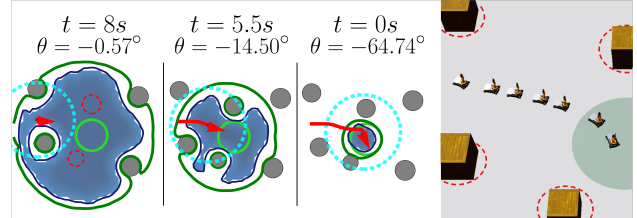


Fig. 1: Preview of finite-time guaranteed contingency planning using Fourier Neural Operator–based Hamilton–Jacobi reachability. The robot state lies within a safe under-approximation (blue) of the true reachable set (green). The final trajectory (red, solid) is obtained by following a gradient-based policy toward the safe set (light green) while avoiding obstacles (grey), which may be unknown (red, dashed) and detected by onboard sensors (cyan). (Rightmost) Realization of the contingency control policy on KUKA’s youBot.

directly synthesizes optimal recovery policies from the value function gradient. However, the prohibitive computational cost of solving the associated PDE has historically limited its use in online planning for unknown environments. Recent advances in learning-based solvers have substantially mitigated this scalability barrier, which enables efficient estimation of HJ reachable sets in real time.

2) *Learning-Based Hamilton Jacobi Reachability*: Recent works approximate the HJI–VI solution using neural PDE solvers trained via residual minimization (e.g., DeepReach [5], ExactBC [6], and physics-informed approaches [7]). These methods learn a fixed PDE instance and require retraining when dynamics, target sets, or horizons change, which limit their use in initially unknown environments. Parametric extensions [8] allow limited variability but remain confined to low-dimensional parameter families. Alternative approaches reformulate reach-avoid problems via discrete-time Bellman operators [9] or classification-based policy learning [10]. While computationally attractive, these methods do not enforce full HJI–VI structural consistency, and safety certification relies on supervisory mechanisms rather than intrinsic PDE guarantees. The work most closely related to ours is HJRNO [11], which employs Fourier Neural Operators to learn the HJ solution operator across varying obstacle configurations. However, it focuses on infinite-horizon invariant sets rather than finite-time reachability and does not provide formal guarantees on the learned safe sets.

3) *Multi-Goal Planning in Obstructed Environments*: Visiting multiple goals optimally is classically formulated as the Traveling Salesman Problem (TSP) (e.g., [12]). In environments with obstacles, this extends to the Physical

The authors are with the Department of Electrical and Computer Engineering, Northeastern University, Boston, MA, USA, 02115 ({muenprasitvej,k,d.aksaray}@northeastern.edu)

¹Videos of the simulated experiment on KUKA’s youBot in Webots simulation can be found at <https://youtu.be/EuYUzjcPtdQ>

TSP (PTSP) [13], where edge costs are induced by motion planning (e.g., RRT* and PRM* [14], SFF* [15], and Lazy-TSP [16]). Existing methods assume prior knowledge of obstacle configurations and do not account for online safety-restricted reachable regions. In contrast, we address contingency-aware multi-goal planning in partially unknown environments, where feasible routing must remain confined to dynamically updated reach-avoid sets.

B. Contributions

This paper presents a unified contingency-aware multi-goal planning framework with certified finite-time reachability guarantees. Our main contributions are:

- 1) We learn *the finite-time* Hamilton–Jacobi–Isaacs variational inequality (HJI-VI) solution operator using a Fourier Neural Operator (FNO) and establish a *theoretical under-approximation* guarantee of the learned reach-avoid sets.
- 2) We propose a resilient framework that integrates FNO-predicted reachable sets into an online multi-goal planner, which allows reactive updates under changing obstacle configurations without resolving the HJI-VI. This framework guarantees that, at every point during execution, the robot maintains a finite-time recovery path to at least one designated safe region under adversarial disturbances.
- 3) We derive a modified gradient-based recovery policy that guarantees finite-time reachability to designated safe regions under adversarial disturbances.
- 4) Finally, we demonstrate the contingency-aware multi-goals planning framework in real-time on KUKA’s youBot in Webots simulation.

II. PRELIMINARIES

A. Hamilton–Jacobi Reachability

We follow the standard HJ reachability formulation [17]. The system state $\mathbf{x} \in \mathcal{X} \subset \mathbb{R}^{n_x}$ evolves as $\dot{\mathbf{x}} = f(\mathbf{x}, \mathbf{u}, \mathbf{d})$, with control $\mathbf{u} \in \mathcal{U} \subset \mathbb{R}^{n_u}$ and disturbance $\mathbf{d} \in \mathcal{D} \subset \mathbb{R}^{n_d}$. Let $\xi_{\mathbf{x},t}^{\mathbf{u},\mathbf{d}}(\tau)$ denote the state reached at time τ starting from initial condition (\mathbf{x}, t) under control $\mathbf{u}(\cdot)$ and disturbance $\mathbf{d}(\cdot)$. Given a target set $\mathcal{L} \in \mathcal{X}$ and unsafe set $\mathcal{G} \in \mathcal{X}$, the backward reach-avoid set (BRAS) over horizon $[t, 0]$ is

$$\mathcal{RA}(t) = \{\mathbf{x} \mid \forall \mathbf{d}, \exists \mathbf{u}, \forall \tau \in [t, 0], \xi_{\mathbf{x},t}^{\mathbf{u},\mathbf{d}}(\tau) \notin \mathcal{G}, \xi_{\mathbf{x},t}^{\mathbf{u},\mathbf{d}}(0) \in \mathcal{L}\},$$

which characterizes all states from which the system can reach \mathcal{L} exactly at $t = 0$ while always avoiding \mathcal{G} .

Let $\mathcal{L} = \{\mathbf{x} \mid \ell(\mathbf{x}) \leq 0\}$ and $\mathcal{G} = \{\mathbf{x} \mid g(\mathbf{x}) \geq 0\}$ for continuous functions $\ell, g : \mathbb{R}^{n_x} \rightarrow \mathbb{R}$. The reach-avoid condition is encoded in cost functional

$$J(\mathbf{x}, t, \mathbf{u}(\cdot), \mathbf{d}(\cdot)) = \max\{\ell(\xi_{\mathbf{x},t}^{\mathbf{u},\mathbf{d}}(0)), \max_{\tau \in [t,0]} g(\xi_{\mathbf{x},t}^{\mathbf{u},\mathbf{d}}(\tau))\},$$

where $J \leq 0$ is the optimality criterion. This yields a zero-sum differential game, and the value function

$$V(\mathbf{x}, t) := \inf_{\mathbf{u}(\cdot)} \sup_{\mathbf{d}(\cdot)} J(\mathbf{x}, t, \mathbf{u}(\cdot), \mathbf{d}(\cdot))$$

is the unique viscosity solution (e.g., [4]) of the HJI variational inequality

$$\max\left\{\partial_t V(\mathbf{x}, t) + \mathcal{H}(\mathbf{x}, \nabla_{\mathbf{x}} V(\mathbf{x}, t)), g(\mathbf{x}) - V(\mathbf{x}, t)\right\} = 0, \quad (1)$$

with terminal condition $V(\mathbf{x}, 0) = \max\{\ell(\mathbf{x}), g(\mathbf{x})\}$ and Hamiltonian

$$\mathcal{H}(\mathbf{x}, t) := \sup_{\mathbf{d} \in \mathcal{D}} \inf_{\mathbf{u} \in \mathcal{U}} \langle \nabla_{\mathbf{x}} V(\mathbf{x}, t), f(\mathbf{x}, \mathbf{u}, \mathbf{d}) \rangle.$$

The BRAS is thus the zero sublevel set $\mathcal{RA}(t) = \{\mathbf{x} \mid V(\mathbf{x}, t) \leq 0\}$, and the optimal feedback control enforcing reachability under worst-case disturbances is

$$\mathbf{u}^*(\mathbf{x}, t) = \arg \min_{\mathbf{u} \in \mathcal{U}} \sup_{\mathbf{d} \in \mathcal{D}} \langle \nabla_{\mathbf{x}} V(\mathbf{x}, t), f(\mathbf{x}, \mathbf{u}, \mathbf{d}) \rangle. \quad (2)$$

B. Fourier Neural Operator

Let $D = (D^{\text{loc}} \times \mathbf{H}) \subset \mathbb{R}^d$ be a bounded open domain with coordinates $(\mathbf{p}, \mathbf{h}) \in D$, where $\mathbf{p} \in D^{\text{loc}}$ denotes spatial variables and $\mathbf{h} \in \mathbf{H}$ denotes parametric variables. Let $\mathcal{A} = \mathcal{A}(D; \mathbb{R}^{d_a})$ and $\mathcal{Y} = \mathcal{Y}(D; \mathbb{R}^{d_y})$ denote separable Banach spaces of functions on D . Given a solution operator $\Psi^\dagger : \mathcal{A} \rightarrow \mathcal{Y}$ associated with a parametric PDE and a finite set of observations $\{a_j, y_j\}_{j=1}^N$, where the inputs a_j are i.i.d. samples on \mathcal{A} and $y_j = \Psi^\dagger(a_j)$, the objective is to approximate Ψ^\dagger by a parametric operator $\Psi_\phi : \mathcal{A} \times \Phi \rightarrow \mathcal{Y}$, where Φ is finite-dimensional and learned from data. The Fourier Neural Operator (FNO) [18] is a mesh-free architecture for approximating solution operators Ψ^\dagger by producing a single set of parameters $\phi \in \Phi$ that generalizes across different discretizations and enables zero-shot super-resolution. Given an input function $a \in \mathcal{A}$, the overall mapping with $B \in \mathbb{N}$ Fourier layers is defined as

$$y = \Psi_\phi(a) := \Pi \circ \text{Layer}_{B-1} \circ \dots \circ \text{Layer}_0 \circ \Lambda(a),$$

where each layer is a latent function taking values in higher dimension \mathbb{R}^{d_v} , and $\Lambda : \mathbb{R}^{d_a} \rightarrow \mathbb{R}^{d_v}$ and $\Pi : \mathbb{R}^{d_v} \rightarrow \mathbb{R}^{d_y}$ denote the lifting and projection operators, respectively. The latent function v_b is defined as

$$v_{b+1}(x) = \text{Layer}_b \doteq \sigma\left(W v_b(x) + \mathcal{F}^{-1}\left(R_\phi \cdot \mathcal{F}(v_b)\right)(x)\right),$$

where $W : \mathbb{R}^{d_v} \rightarrow \mathbb{R}^{d_v}$ is a pointwise linear map, σ is an activation function, \mathcal{F} and \mathcal{F}^{-1} are the Fourier transform and its inverse respectively, and R_ϕ is a learned tensor that parameterizes the kernel in the Fourier domain via pointwise spectral multiplication.

Theorem 1 (Universal Approximation by FNO). *Let \bar{D} be a compact domain with Lipschitz boundary, and let $\Psi^\dagger : \mathcal{F} \rightarrow \mathcal{F}'$ be a continuous operator between function spaces on \bar{D} . For any $\varepsilon > 0$ and compact $\mathcal{K} \subset \mathcal{F}$, there exists a nonlocal FNO $\Psi_\phi : \mathcal{F} \rightarrow \mathcal{F}'$ such that*

$$\sup_{g \in \mathcal{K}} \|\Psi^\dagger(g) - \Psi_\phi(g)\|_{\mathcal{F}'} \leq \varepsilon,$$

where the true operator Ψ^\dagger maps $\mathbb{C}^s(\bar{D}; \mathbb{R}) \rightarrow \mathbb{C}^{s'}(\bar{D}; \mathbb{R})$ in continuous function spaces, or $\mathbb{W}^{s,p}(\bar{D}; \mathbb{R}) \rightarrow \mathbb{W}^{s',p'}(\bar{D}; \mathbb{R})$ in Sobolev spaces, with $s, s' \geq 0$ and $p, p' \in [1, \infty)$.

Proof. This result follows directly from [19, Theorem 5 and 9] [20, Theorem 1–2]. \square

III. PROBLEM DEFINITION

Consider a mobile robot navigating in a 2D planar environment $\Omega \subset \mathbb{R}^2$ with $L \in \mathbb{N}$ pre-defined safe sets $\mathbf{L} = \{\mathcal{L}_i^G\}_{i=1}^L \subset \Omega$ centered at $\mathbf{p}_{\ell_i} \doteq (x_{\ell_i}, y_{\ell_i}) \in \mathbb{R}^2$ and $H \in \mathbb{N}$ unknown obstacles $\mathbf{O} = \{\mathcal{O}_j\}_{j=1}^H \subset \Omega$ centered at $\mathbf{p}_{\mathcal{O}_j} \doteq (x_{\mathcal{O}_j}, y_{\mathcal{O}_j}) \in \mathbb{R}^2$. For each safe set \mathcal{L}_i^G ,² we define the unsafe set as $\mathcal{G}_i^G = \bigcup_j \mathcal{O}_j$ for all \mathcal{O}_j within the local vicinity D_i^{loc} of \mathcal{L}_i^G , where $D_i^{\text{loc}} \subset \mathbb{R}^2$.

Let a mobile robot governed by continuous dynamics $\dot{\mathbf{x}} = f(\mathbf{x}, \mathbf{u}, \mathbf{d})$, where $\mathbf{x}(t) \doteq (\mathbf{p}_{\text{robot}}, \theta) \in \mathcal{X} \subset \mathbb{R}^3$ represents robot’s position $\mathbf{p}_{\text{robot}} \doteq (x, y) \in \mathbb{R}^2$ and orientation $\theta \in \mathbb{S}^1$ at time $t \in \mathbb{R}_{\geq 0}$, $\mathbf{u}(t) \in \mathcal{U} \subset \mathbb{R}^{n_u}$ is the control input, and $\mathbf{d}(t) \in \mathcal{D} \subset \mathbb{R}^{n_d}$ is the disturbance. The robot is equipped with omnidirection sensor of radius $r_{\text{sense}} > 0$ which can detect an obstacle at $\mathbf{p}_{\mathcal{O}_i}$ if $\|\mathbf{p}_{\mathcal{O}_i} - \mathbf{p}_r\| \leq r_{\text{sense}}$. We now state the following assumption regarding \mathcal{L}^G and \mathcal{G}^G .

Assumption 1. *The safe set $\mathcal{L}^G \subset \Omega$ is a closed disk of radius $r_\ell > 0$ centered at \mathbf{p}_ℓ , i.e., $\mathcal{L}^G = \{\mathbf{p} \in \mathbb{R}^2 : \|\mathbf{p} - \mathbf{p}_\ell\| \leq r_\ell\}$. If detected, each obstacle $\mathcal{O}_j \subset \Omega$ is approximated as a closed disk of radius $r_{\mathcal{O}_j} > 0$ centered at $\mathbf{p}_{\mathcal{O}_j}$, such that $\mathcal{G}^G = \bigcup_i \mathcal{O}_i$. Furthermore, all obstacles are assumed to be disjoint from the safe set, i.e., $\|\mathbf{p}_{\mathcal{O}_j} - \mathbf{p}_\ell\| > r_{\mathcal{O}_j} + r_\ell$, $\forall \mathcal{O}_j \in D^{\text{loc}}$, which ensures $\mathcal{L} \cap \mathcal{G} = \emptyset$.*

Problem Statement: Under Assumption 1, given a planar environment Ω containing H unknown obstacles \mathbf{O} and L sufficiently overlapping, formally certified safe sets \mathbf{L} , a robot with dynamics $\dot{\mathbf{x}} = f(\mathbf{x}, \mathbf{u}, \mathbf{d})$ must accomplish the following: (i) visit $K \geq 1$ goal locations $\mathbf{P}_{\text{goals}} = \{\mathbf{p}_{\text{goal}_k}\}_{k=1}^K$ in a locally optimal sequence non-intersecting with \mathbf{O} and (ii) at every state \mathbf{x} along the planned path, finite-time reachability to at least one certified safe set $\mathcal{L}_i^G \in \mathbf{L}$ is guaranteed—such that a reachability-based contingency policy remains available throughout execution.

IV. PROPOSED METHOD

Running Example (Unicycle): In this work, we consider the unicycle model with additive disturbance. The state is $\mathbf{x} = (x, y, \theta) \in \mathcal{X}$, the control is $\mathbf{u} = (v, \omega) \in \mathcal{U}$, and the disturbance is $\mathbf{d} = (d_x, d_y, d_\theta) \in \mathcal{D}$:

$$\dot{x} = v \cos \theta + d_x, \quad \dot{y} = v \sin \theta + d_y, \quad \dot{\theta} = \omega + d_\theta, \quad (3)$$

where $v \in [v_{\min}, v_{\max}]$, $\omega \in \omega_{\max}[-1, 1]$ with $v_{\min} \geq 0$, and disturbance set satisfies $\|(d_x, d_y)\|_2 \leq \bar{d}$, $d_\theta \in [-\bar{d}_\theta, \bar{d}_\theta]$.

Additionally, (3) is uniformly Lipschitz continuous in \mathbf{x} , satisfying $\|f(\mathbf{x}, \mathbf{u})\|_2 = \sqrt{v^2 + \omega^2} \leq \sqrt{v_{\max}^2 + \omega_{\max}^2}$.

²The superscript G denotes quantities expressed in the global coordinate frame. It is applied only to \mathcal{L} and \mathcal{G} , as these sets are originally defined in the local domain D^{loc} and then mapped to the global frame. Other variables directly defined in the global frame do not require this superscript.

A. Operator Learning for HJI-VI

Inspired by [11], we implement the FNO architecture of Sec. II-B to learn the solution operator Ψ_ϕ of HJI-VI (1), enabling zero-shot super-resolution of the reachable set. Ψ_ϕ maps the obstacle configuration $g(\mathbf{x})$ and time constant t to the viscosity solution $V^\dagger(\mathbf{x}, t)$; thus the solution characterizes t -horizon BRAS. Hereafter, the superscript \dagger denotes the true solution and subscript ϕ the learned approximation.

The safe set is defined over the compact state set \mathcal{X} as

$$\mathcal{L} := \{\mathbf{x} \doteq (\mathbf{p}, \theta) \in \mathcal{X} \mid \|\mathbf{p}\|_2 \leq r_\ell\}, \quad (4)$$

i.e., a closed cylinder of radius r_ℓ centered at the origin.

For the i -th obstacle with center $\mathbf{p}_{\mathcal{O}_i}$ and radius $r_{\mathcal{O}_i}$, define $g_i(\mathbf{x}) = r_{\mathcal{O}_i} - \|\mathbf{p} - \mathbf{p}_{\mathcal{O}_i}\|_2$, so $g_i \geq 0$ characterizes its interior. Given at most H observed obstacles, the unsafe set is

$$\mathcal{G} := \{\mathbf{x} \doteq (\mathbf{p}, \theta) \in \mathcal{X} \mid g(\mathbf{x}) \geq 0\}, \quad (5)$$

where $g(\mathbf{x}) = \max_{1 \leq i \leq H} g_i(\mathbf{x})$ encodes the union of all obstacles via point-wise maximum.

As in [11], we parameterize $(x, y) \in D^{\text{loc}} \subset \mathbb{R}^2$ as the primary input domain and treat the remaining state as hyperparameter. We further extend this formulation by introducing time as an additional hyperparameter to explicitly capture finite-time reachability. Specifically, the hyperparameter vector is defined as $(\theta, t) \in \mathbf{h} \subset \mathbb{S}^1 \times \mathbb{R}_{\geq 0}$. Under this representation, the learning problem is formulated as

$$a(\mathbf{x}) = g(x, y, \mathbf{h}), \quad y(\mathbf{x}) = V(x, y, \mathbf{h}).$$

We omit \mathcal{L} from the inputs since it is fixed across all training instances, and the network implicitly encodes it through training.

The training dataset is generated using `toolboxLS` and `helperOC` [21], which numerically solve (1) on a coarse spatial grid over discrete time instances, yielding $\mathcal{S}_{\text{train}} = \{(g_j(x, y, \mathbf{h}), V_j^\dagger(x, y, \mathbf{h}))\}_{j=1}^N$, where each pair corresponds to a 2D spatial slice of the obstacle signed distance field $g(x, y, \theta_j)$ and viscosity solution $V^\dagger(x, y, \theta_j, t_j)$ evaluated at hyperparameter pair (θ_j, t_j) . Sampling and aggregating across the hyperparameter domain hence yields an approximated solutions $V_\phi(\mathbf{x}, t)$ to (1). The FNO model is trained by minimizing

$$\min_{\phi} \frac{1}{N} \sum_{j=1}^N (1 - \lambda) \|e_j\|_\infty + \lambda \|e_j\|_2, \quad (6)$$

where $e_j := V_j^\dagger(x, y, \mathbf{h}) - \Psi_\phi(g_j(x, y, \mathbf{h}))$, the L^∞ term penalizes the worst-case value error, the L^2 term regulates the average pointwise error for training stability, and $\lambda \in [0, 1]$.

B. Safety Guarantees for FNO-based HJ Reachability

Given dynamics (3) and definitions (4) and (5), $f(\mathbf{x}, \mathbf{u}, \mathbf{d})$, $\ell(\mathbf{x})$ and $g(\mathbf{x})$ are bounded, Lipschitz continuous in \mathbf{x} , and continuous in \mathbf{u} and \mathbf{d} . Thus, $V^\dagger(\mathbf{x}, t)$ is a bounded, Lipschitz continuous function [4]. By Rademacher’s theorem, $V^\dagger(\mathbf{x}, t)$ is differentiable almost everywhere (a.e.) in (\mathbf{x}, t) -space [22, Theorem 3.2].

In FNO setting, let $\bar{D} = D^{\text{loc}} \cup \mathbf{h} = \mathcal{X} \times [0, T]$ be a compact domain. Define $\Psi^\dagger(g(\mathbf{x}), t) := V^\dagger(\mathbf{x}, t)$ and hence the FNO model Ψ_ϕ is approximating a solution operator mapping $\mathbb{C}^0(\bar{D}; \mathbb{R}) \rightarrow \mathbb{C}^0(\bar{D}; \mathbb{R})$ as well as $\mathbb{W}^{1,\infty}(\bar{D}; \mathbb{R}) \rightarrow \mathbb{W}^{1,2}(\bar{D}; \mathbb{R})$. We now state the following assumptions:

Assumption 2. *Let the FNO model Ψ_ϕ with large enough B Fourier Layers be sufficiently trained via (6), such that for some $\varepsilon, \varepsilon_0 > 0$ it satisfies universal approximation in Th. 1:*

$$\|V_\phi(\mathbf{x}, t) - V^\dagger(\mathbf{x}, t)\|_\infty \leq \varepsilon, \text{ and}$$

$$\|\nabla_{\mathbf{x}} V_\phi - \nabla_{\mathbf{x}} V^\dagger\|_{L^2} \leq \|V_\phi(\mathbf{x}, t) - V^\dagger(\mathbf{x}, t)\|_{\mathbb{W}^{1,2}} \leq \varepsilon_0,$$

where $V^\dagger(\mathbf{x}, t) := \Psi^\dagger(g(\mathbf{x}), t)$ and $V_\phi(\mathbf{x}, t) := \Psi_\phi(g(\mathbf{x}), t)$.

On compact subsets of the domain, Th. 1 guarantees that any continuous operator between appropriate function spaces can be approximated arbitrarily well by an FNO. Assumption 2 postulates that the trained model Ψ_ϕ used in our framework attains this approximation accuracy, satisfying the error bounds ε and ε_0 . Thus, $\varepsilon \rightarrow 0$ implies pointwise convergence on $\mathcal{X} \times [0, T]$. Since convergence in $\mathbb{W}^{1,2}$ implies convergence of the gradients in L^2 , $\varepsilon_0 \rightarrow 0$ ensures that the gradient error vanishes in the mean-square sense.

Under Assumption 2, we now provide Lem. 1 which establishes FNO underapproximation of the true reach-avoid set. Then Corollary 1 establishes a translation invariance property of BRAS. This property allows the FNO model Ψ_ϕ , which is trained over the local domain D^{loc} , to be deployed in the global environment Ω for our planning framework.

Lemma 1 (ε -Sublevel Set Underapproximation). *Given any signed distance function $g(\mathbf{x})$ defined over the $\mathcal{X} \times [0, T]$, define the true and predicted reachable sets as $\mathcal{RA}^\dagger(t) := \{\mathbf{x} \in \mathcal{X} : V^\dagger(\mathbf{x}, t) \leq 0\}$ and $\mathcal{RA}_\phi(t) := \{\mathbf{x} \in \mathcal{X} : V_\phi(\mathbf{x}, t) \leq 0\}$, respectively. Then the ε -sublevel of the learned set*

$$\mathcal{RA}_\phi^\varepsilon(t) := \{\mathbf{x} \in \mathcal{X} : V_\phi(\mathbf{x}, t) \leq -\varepsilon\} \quad (7)$$

satisfies the under-approximation $\mathcal{RA}_\phi^\varepsilon(t) \subset \mathcal{RA}^\dagger(t)$.

Proof. Since $\mathcal{X} \times [0, T]$ is compact, Assumption 2 guarantees a uniform L^∞ error bound on the FNO-approximation $\|V^\dagger(\mathbf{x}, t) - V_\phi(\mathbf{x}, t)\|_\infty \leq \varepsilon$. Hence, $V^\dagger(\mathbf{x}, t) \leq V_\phi(\mathbf{x}, t) + \varepsilon$ in the worst case. If $\mathbf{x} \in \mathcal{RA}_\phi^\varepsilon(t)$, then $V_\phi(\mathbf{x}, t) \leq -\varepsilon$, and therefore $V^\dagger(\mathbf{x}, t) \leq -\varepsilon + \varepsilon = 0$, which implies $\mathbf{x} \in \mathcal{RA}^\dagger(t)$. The uniform value closeness guarantees that the ε -shifted learned sublevel set lies entirely within the true reachable set, thereby certify finite-time reachability property of the learned set. \square

Corollary 1. *Let $V_\phi(x, y, \theta', t)$ denote a θ' -slice of the value function defined on $(x, y) \in D^{\text{loc}}$ associated with the safe set \mathcal{L} in (4). For a safe set \mathcal{L}^G centered at $\mathbf{p}_\ell = (x_\ell, y_\ell)$ in the global frame, the value function is obtained by spatial translation: $V_\phi^G(x, y, \theta', t) = V_\phi(x - x_\ell, y - y_\ell, \theta', t)$. This translation preserves the reachability property, i.e., $V_\phi^G(x, y, \theta', t) \leq -\varepsilon \iff (x, y, \theta') \in \mathcal{RA}_\phi^\varepsilon(t) \subset \mathcal{RA}^\dagger(t)$ for all $(x - x_\ell, y - y_\ell) \in D^{\text{loc}}$ and $t \in [0, T]$.*

As mentioned in footnote 2, the safe set \mathcal{L}^G centered at $\mathbf{p}_\ell \in \Omega$ is a spatial translation of \mathcal{L} centered at the origin. The corresponding value function is $V^G(\mathbf{p}, \theta, t) = V(\mathbf{p} - \mathbf{p}_\ell, \theta, t)$. The associated unsafe set \mathcal{G}^G is defined with $g^G(\mathbf{x}) = g(\mathbf{p} - \mathbf{p}_\ell)$, where each obstacle $\mathcal{O} \in \Omega$ is translated by $(\mathbf{p}_\mathcal{O} - \mathbf{p}_\ell)$ into D^{loc} , for all $\mathbf{p} \in \Omega \subset \mathbb{R}^2$.

C. Contingency-Aware Multi-Goal Planning Framework

1) *RRT^X and Traveling Salesman Problem:* Before presenting the full algorithm, we first outline the key components underlying our approach. RRT^X [23] maintains a state-space graph $\text{Gr} = (\mathcal{V}, \mathcal{E})$ with vertex set \mathcal{V} , edge set \mathcal{E} , and a shortest-path tree $\text{Tr} \subseteq \text{Gr}$ rooted at \mathbf{p}_{goal} . Each vertex $\mathbf{p} \in \text{Tr}$ stores a parent pointer encoding its least-cost path to \mathbf{p}_{goal} and a cost-to-goal $c_{\text{Tr}}(\mathbf{p})$, with $c_{\text{Tr}}(\mathbf{p}) = \infty$ if $\mathbf{p} \notin \text{Tr}$. As a variant of RRT* [14], it inherits the same asymptotic optimality conditions but roots Tr at \mathbf{p}_{goal} , enabling direct cost propagation from the goal. When an unknown obstacle is detected, each invalidated vertex searches its running neighborhood $\mathcal{N}_r(\mathbf{p})$ for the lowest-cost parent candidate and triggers a local rewiring cascade until all of the best available parents are connected to Tr . We refer the reader to [23] for further details. Given a separate tree Tr_i rooted at each $\mathbf{p}_{\text{goal}_i} \in \mathbf{P}_{\text{goals}}$, the inter-goal cost $c_{ij} = c_{\text{Tr}_j}(\mathbf{p}_{\text{goal}_i})$ is read directly from each tree. These costs form an asymmetric TSP solved via the Bellman–Held–Karp algorithm [24], which produces globally optimal visitation order $\mathbf{P}_{\text{goals}}(\sigma^*)$, where σ^* is the optimal permutation index over $\mathbf{P}_{\text{goals}}$.

Together, the local rewiring of RRT^X and the zero-shot super-resolution of the FNO form a tightly coupled update mechanism: upon detecting a new obstacle, the FNO rapidly recomputes the high-resolution reachable set, and RRT^X propagates the induced cost changes locally instead of global replanning. The resulting planner (Alg. 1) optimally visits $K \geq 1$ goals while adapting efficiently to dynamic obstacles.

2) *Reachability Constraint for Nominal Planner:* To ensure contingency behaviour is enforced throughout nominal mission, we propose a reachability constraint on the planning space, which guarantees finite-time reachability to at least one safety region $\mathcal{L}_i^G \in \mathbf{L}$ at every state for all times.

Let $V_\phi^G(x, y, \theta, T)$ denote the value function at time T for safe set \mathcal{L}^G centered at $\mathbf{p}_\ell = (x_\ell, y_\ell)$. Define the heading-agnostic value function as a point-wise minimum over θ :

$$\bar{V}_\phi^G(x, y, T) := \min_{\theta \in \Theta} V_\phi^G(x, y, \theta, T), \quad (8)$$

with BRAS: $\bar{\mathcal{RA}}_\phi^\varepsilon(T) = \{(x, y) \in \Omega \mid \bar{V}_\phi^G(x, y, T) \leq -\varepsilon\}$.

For simplicity, given the i^{th} safe set \mathcal{L}_i^G , denote the T -time 2D BRAS as $\Omega_{\text{reach}_i} = \bar{\mathcal{RA}}_{\phi,i}^\varepsilon(T)$. For an environment Ω with safe sets $\mathbf{L} = \{\mathcal{L}_i^G\}_{i=1}^L$, we define the feasible planning region as $\Omega_{\text{feasible}} := \bigcup_{i=1}^L \Omega_{\text{reach}_i}$. Note that by definitions (7) and (8), the inclusion $\bar{\mathcal{RA}}_\phi^\varepsilon(T) \subset \mathcal{RA}_\phi^\varepsilon(T) \subset \mathcal{RA}^\dagger(T)$ holds. This ensures that Ω_{feasible} is a valid conservative feasible region for nominal planning that is agnostic to robot's orientation and guarantees reachability toward the safe set within finite-time T . Visualization is provided in Fig. 2.

Algorithm 1: Contingency-Aware Multi-Goals Planning Algorithm

Input: FNO models $\{\Psi_{\phi_l}\}_{l=1}^L$, Set of safe regions $\mathbf{L} = \{\mathcal{L}_l^G\}_{l=1}^L$, Set of goal locations $\mathbf{P}_{\text{goals}}$, Set of unknown obstacles $\mathbf{O} = \{\mathcal{O}_h\}_{h=1}^H$

- 1 $\mathbf{O}_{\text{known}} \leftarrow \emptyset$;
- 2 $\{\text{Tr}_k\}_{k=1}^K \leftarrow \text{RRT}^X \{\text{Gr}_k\}_{k=1}^K$ rooted at $\{\mathbf{p}_{\text{goal},k}\}_{k=1}^K$;
- 3 $\mathbf{x} \leftarrow (\mathbf{p}_{\text{goal}_1}, \theta)$; // robot starts at goal 1
- 4 $\sigma^* \leftarrow$ Optimal tour [24] on $\mathbf{P}_{\text{goals}}$;
- 5 $\Omega_{\text{feasible}} = \bigcup_{l=1}^L \Omega_{\text{reach}_l} \leftarrow \bigcup_{l=1}^L \Psi_{\phi_l}(g_h)$;
- 6 **for** $i = 2, \dots, K$ **do**
- 7 **while** $\mathbf{p}_{\text{robot}} \neq \mathbf{P}_{\text{goals}}(\sigma_i^*)$ **do**
- 8 $\sigma_{\text{rem}} = \{\sigma_j^*\}_{j=i}^K$; // unvisited indices
- 9 $\sigma_{\text{invalid}} = \emptyset$; // unreachable indices
- 10 $\text{Tr}_{\sigma_i^*} \leftarrow \text{RRT}^X$ extending $\text{Gr}_{\sigma_i^*}$ [23, Alg. 1];
- 11 $\mathbf{x} = (\mathbf{p}_{\text{robot}}, \theta) \leftarrow f(\mathbf{x}, \mathbf{u}_{\mathbf{p}})$, $\mathbf{u}_{\mathbf{p}} = \mathbf{u}(\text{Tr}_{\sigma_i^*})$;
- 12 $\mathbf{O}_{\text{new}} \leftarrow \{\mathcal{O}_h \in \mathbf{O} \setminus \mathbf{O}_{\text{known}} \mid \|\mathbf{p}_{\mathcal{O}_h} - \mathbf{p}_{\text{robot}}\| \leq r_{\text{sense}}\}$;
- 13 **if** $\mathbf{O}_{\text{new}} \neq \emptyset$ **then**
- 14 $\mathbf{O}_{\text{known}} \leftarrow \mathbf{O}_{\text{known}} \cup \mathbf{O}_{\text{new}}$;
- 15 $\Omega_{\text{feasible}} \leftarrow \bigcup_l \Psi_{\phi_l}(g_h)$, $\forall \mathcal{L}_l^G \in \mathbf{L}, \exists \mathcal{O}_h \in \mathbf{O}_{\text{new}}$
s.t. $D_l^{\text{loc}} \cap \mathcal{O}_h \neq \emptyset$;
- 16 **for** $k \in \sigma_{\text{rem}}$ **do**
- 17 $\text{Tr}_k \leftarrow \text{RRT}^X$ rewiring cascade [23, Alg. 8] s.t.
 $\text{Tr}_k \in \Omega_{\text{feasible}} \setminus \mathbf{O}_{\text{known}}$;
- 18 **if** $\mathbf{p}_{\text{robot}} \notin \text{Tr}_k$ **then**
- 19 $\sigma_{\text{invalid}} = \sigma_{\text{invalid}} \cup \{k\}$;
- 20 $\sigma_{\text{rem}}^* \leftarrow$ Optimal tour [24] on $\mathbf{p}_{\text{robot}} \cup \mathbf{P}_{\text{goals}}(\sigma_{\text{rem}})$;
- 21 $\sigma^* \leftarrow \{\sigma_1, \dots, \sigma_{i-1}, \sigma_{\text{rem}}^*\}$;
- 22 **if** $\text{adversary} \vee (\sigma_{\text{rem}} = \sigma_{\text{invalid}})$ **then**
- 23 $l^* \leftarrow \arg \min_{l \in \{0, \dots, L\}} V_{\phi_l}^G(\mathbf{x}, t)$;
- 24 **while** $\mathbf{p}_{\text{robot}} \notin \mathcal{L}_{l^*}^G$ **do**
- 25 $\mathbf{u}^* \leftarrow$ Contingency policy (9);
- 26 $\mathbf{x} = (\mathbf{p}_{\text{robot}}, \theta) \leftarrow f(\mathbf{x}, \mathbf{u}^*)$;
- 27 **for** $k \in \sigma_{\text{invalid}}$ **do**
- 28 $\text{Tr}_k \leftarrow \text{RRT}^X$ extending Gr_k [23, Alg. 1];

Additionally, we impose a *sufficient overlap* condition on the adjacent reachable sets to enable the nominal planner to extend across the two sets.

Lemma 2 (Sufficient Overlap of Reachable Sets). *Let \mathcal{L}_i^G and \mathcal{L}_j^G be safe sets centered at \mathbf{p}_{ℓ_i} and \mathbf{p}_{ℓ_j} with associated reachable regions Ω_{reach_i} and Ω_{reach_j} , respectively. Let $\delta > 0$ denote the maximum step length of a nominal planner. A sufficient condition for the planner to admit extensions across Ω_{reach_i} and Ω_{reach_j} is:*

$$\exists \mathbf{p}_0 \in \Omega_{\text{reach}_i} \cap \Omega_{\text{reach}_j} \text{ s.t. } B_\delta(\mathbf{p}_0) \subseteq \Omega_{\text{reach}_i} \cap \Omega_{\text{reach}_j},$$

where $B_\delta(\mathbf{p}_0) := \{\mathbf{p} \in \mathbb{R}^2 \mid \|\mathbf{p} - \mathbf{p}_0\|_2 \leq \delta\}$ is the closed Euclidean ball of radius δ centered at \mathbf{p}_0 .

Proof. The existence of $B_\delta(\mathbf{p}_0) \subseteq \Omega_{\text{reach}_i} \cap \Omega_{\text{reach}_j}$ guarantees that any state within $B_\delta(\mathbf{p}_0)$ can be connected to \mathbf{p}_0 in a single step of size δ , while remaining within the overlap region. Visualization is provided in Fig. 2. \square

3) *Overall Algorithm:* Alg. 1 initializes with L offline-trained FNO models Ψ_{ϕ_l} corresponding to the safe set \mathcal{L}_l^G . The safe sets are positioned such that their predicted reachable sets are *sufficiently overlap* satisfying Lem. 2 and collectively defines Ω_{feasible} . If there are no known obstacles initially, true reachable set may be computed offline once. We modify the RRT^X algorithm such that the graph Gr remains confined within the dynamically updated BRAS, which restricts planning to the feasible subset $\Omega_{\text{feasible}} \subset \Omega$. During node extension, samples are drawn from a mixture

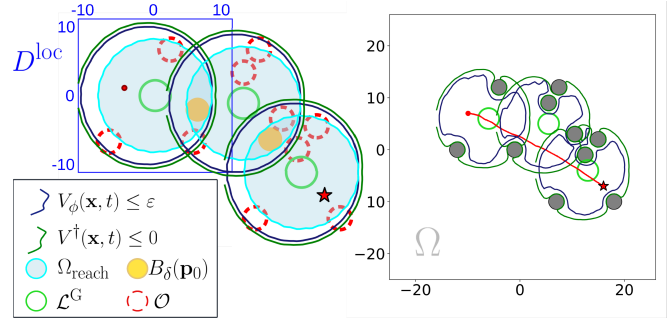


Fig. 2: Overview of the planning framework in Alg. 1 with $K = 1$ goal (red star) and initially unknown obstacles (red, dashed). The ε -sublevel set of the FNO-predicted reachable set (dark blue) is guaranteed to under-approximate the true reachable set (green). The FNO model is trained over a local domain D^{loc} (blue) and integrated into planning within the global environment Ω (grey). Prior to planning, the heading-agnostic reachable sets (cyan) must sufficiently overlap to contain a closed Euclidean ball (yellow), ensuring feasibility of the nominal planner with step length δ across adjacent sets. The final trajectory toward the goal is shown in red.

of 2D Gaussian distributions centered at the safe-set representatives \mathbf{p}_{ℓ_i} . Within Ω_{feasible} , the shortest-path subtree Tr_k is initialized and rooted at each $\mathbf{p}_{\text{goal}_k} \in \mathbf{P}_{\text{goals}}$. This induces an asymmetric TSP over $\mathbf{P}_{\text{goals}}$ with edge costs $c_{i,j} = c_{\text{Tr}_j}(\mathbf{p}_{\text{goal}_i})$. If the robot's initial state does not coincide with any goal, it is appended to $\mathbf{P}_{\text{goals}}$ with its own subtree Tr . The Held-Karp program is then solved with the robot designated as $\mathbf{p}_{\text{goal}_1}$ (Lines 1–5).

The robot executes the optimal visiting sequence with $\sigma_{\text{rem}} = (\sigma_2^*, \dots, \sigma_K^*)$ initially. For each $\sigma_i^* \in \sigma_{\text{rem}}$, the robot traverses along $\text{Tr}_{\sigma_i^*}$ toward $\mathbf{P}_{\text{goals}}(\sigma_i^*)$ via the tracking controller $\mathbf{u}_{\mathbf{p}} = \mathbf{u}(\text{Tr}_{\sigma_i^*})$, where $\mathbf{u}_{\mathbf{p}} \doteq (v_{\mathbf{p}}, \omega_{\mathbf{p}})$ is resolved geometrically from the planned path subject to (3). Concurrently, $\text{Gr}_{\sigma_i^*}$ continues to grow, maintaining RRT^* -like optimal-cost rewiring from $\mathbf{P}_{\text{goals}}(\sigma_i^*)$ to the current robot position $\mathbf{p}_{\text{robot}}$ and all remaining $K - 1$ goals. Note that RRT^X accommodates arbitrary kinodynamic constraints other than (3), and Ψ_{ϕ} is adaptable to other robot dynamics given availability of training data (Lines 6–11).

Upon sensing unknown obstacles $\mathbf{O}_{\text{new}} \subset \mathbf{O}$ (Line 13), two updates are triggered. First, for each $\mathcal{O}_h \in \mathbf{O}_{\text{new}}$ within the local frame D_l^{loc} of the safe set \mathcal{L}_l^G centered at \mathbf{p}_{ℓ_l} , the FNO Ψ_{ϕ_l} predicts a new reachable set $\mathcal{R}_{\mathcal{A}_{\phi_l}^\varepsilon}$ given the updated input $g_h = \max\{g_h, g_{\text{new}}\}$, where $g_{\text{new}} = r_{\mathcal{O}_h} - \|\mathbf{p} - \mathbf{p}_{\mathcal{O}_h}\|_2$ is defined over $(\mathbf{p} - \mathbf{p}_{\ell_l}) \in D_l^{\text{loc}}$. Second, all K subtrees are updated via the RRT^X rewiring cascade [23, Alg. 8] over the updated feasible planning space Ω_{feasible} . During the i -th goal visitation, trees Tr_k with $k \in \sigma_{\text{rem}} \setminus \{\sigma_i^*\}$ do not grow concurrently during robot execution, so a path in Tr_k reaching $\mathbf{p}_{\text{robot}}$ may not exist. Such trees are marked invalid via σ_{invalid} , and the nearest node $\mathbf{q}_{\text{near}} \in \text{Gr}_k$ with $\mathbf{p}_{\text{robot}} \in \mathcal{N}_r(\mathbf{q}_{\text{near}})$ is stored for subsequent rewiring. If no such node exists, Gr_k is grown with increased bias toward $\mathbf{p}_{\text{robot}}$ during replanning. Upon any graph change, Held-Karp is re-solved to obtain a new visiting sequence from the robot's current position $\mathbf{p}_{\text{robot}}$, designated as index 1,

over the remaining goals $\mathbf{P}_{\text{goals}}(\sigma_{\text{rem}})$. Since $\mathbf{p}_{\text{robot}}$ is no longer a root node of a tree, we encode infeasible transition as $c_{ij} = \infty$ in two cases: (i) $i \neq j = 1$, since no path from $\mathbf{p}_{\text{goal}_i}$ to $\mathbf{p}_{\text{robot}}$ exists, and (ii) $i = 1, j \in \sigma_{\text{invalid}}$, since that goal is temporarily unreachable. This yields a minimum-cost feasible sequence σ_{rem}^* consistent with the current obstacle configuration, ensuring reactive and locally optimal decision-making throughout the mission (Lines 13–21).

Upon an adversarial encounter (*adversary*) or when no valid subtree remains, the contingency policy of Sec. IV-D is invoked. The robot is then directed toward the l^* -th safe set $\mathcal{L}_{l^*}^G \in \mathbf{L}$, selected as the one with the smallest $V_\phi(\mathbf{x}, t)$ at $\mathbf{p}_{\text{robot}}$. Since $\mathbf{p}_{\text{robot}} \in \Omega_{\text{feasible}}$, the safe under-approximation (Lem. 1) and translation invariance (Corollary 1) guarantee reachability of $\mathcal{L}_{l^*}^G$ in finite time T whenever $V_{\phi_{l^*}}^G(\mathbf{x}, t) \leq \varepsilon$. Upon reaching $\mathcal{L}_{l^*}^G$, the robot enters a safe dwell period during which any invalidated subtrees are replanned (Lines 22–28).

D. Reachability-based Contingency Policy

In the event of an adversary during nominal planning, we propose a finite-time reachability-based contingency policy that drives the system toward \mathcal{L} while avoiding \mathcal{G} under worst-case disturbance. The analysis is considered with respect to the local state domain $\mathbf{x} \in \mathcal{X}$ over time horizon $t \in [0, T]$. To ensure the policy guides the robot toward the safe set, we augment the FNO-predicted value function V_ϕ to satisfy the two conditions implied by the HJI-VI: $V_\phi(\mathbf{x}, t) \geq g(\mathbf{x})$ and $\partial_t V_\phi(\mathbf{x}, t) + \mathcal{H}(\mathbf{x}, \nabla_{\mathbf{x}} V_\phi(\mathbf{x}, t)) \leq 0$.

1) *Guarantees on obstacle avoidance*: The HJI-VI (1) requires $V^\dagger(\mathbf{x}, t) \geq g(\mathbf{x})$ for all (\mathbf{x}, t) . To impose this on V_ϕ , we project it onto the admissible set at each time t by $\tilde{V}_\phi(\mathbf{x}, t) = \max\{V_\phi(\mathbf{x}, t), g(\mathbf{x})\}$ for all $(\mathbf{x}, t) \in \mathcal{X} \times [0, T]$, following [4]. This enforces $\tilde{V}_\phi(\mathbf{x}, t) \geq g(\mathbf{x})$ pointwise, ensuring $\nabla_{\mathbf{x}} \tilde{V}_\phi$ is consistent with the obstacle boundary and does not induce descent into the unsafe sets.

2) *Reaching terminal state*: To enforce the reach condition, we additionally require \tilde{V}_ϕ to satisfy the HJI-VI residual $\mathbf{D}_t(\mathbf{x}, t) := \partial_t \tilde{V}_\phi(\mathbf{x}, t) + \mathcal{H}(\mathbf{x}, \nabla_{\mathbf{x}} \tilde{V}_\phi(\mathbf{x}, t)) \leq 0$ for all (\mathbf{x}, t) , ensuring \tilde{V}_ϕ remains a viscosity subsolution of (1) along the reaching trajectory.

To enforce the reach condition, we define the violation set $D_{\text{violate}} := \{(\mathbf{x}, t) \in \mathcal{X} \times [0, T] : \mathbf{D}_t(\mathbf{x}, t) > 0\}$ where \tilde{V}_ϕ fails to satisfy the HJI-VI. For a well-trained Ψ_ϕ satisfying Assumption 2 with $\|\nabla_{\mathbf{x}} V_\phi - \nabla_{\mathbf{x}} V^\dagger\|_{L^2(\mathcal{X})} \leq \varepsilon_0$, we first show that D_{violate} is measure-theoretically negligible for small ε_0 . Letting $e = V_\phi - V^\dagger$ and assuming the true solution (away from the switching surface) satisfies strict descent $\mathbf{D}_t(\mathbf{x}, t) \leq -\alpha_0$, the uniform bound $\|f(\mathbf{x}, \mathbf{u}, \mathbf{d})\| \leq M_f = \sqrt{v_{\text{max}}^2 + \omega_{\text{max}}^2}$ on dynamics (3) implies $\mathcal{H}(\mathbf{x}, p)$ is Lipschitz in p with constant M_f , which yields $|\mathbf{D}_t(\mathbf{x}, t)| \leq |\partial_t e| + M_f \|\nabla_{\mathbf{x}} e\|$. The temporal derivative error is empirically subdominant to the spatial gradient term, satisfying $|\partial_t e| \leq \rho M_f \|\nabla_{\mathbf{x}} e\|$ with $\rho < 1$. Hence a violation requires $\|\nabla_{\mathbf{x}} e\| > \alpha_0 / (M_f(1 + \rho))$, and applying the Chebyshev inequality [25, Chapter 6.3] yields $\text{meas}(D_{\text{violate}}) \leq (1 + \rho)^2 M_f^2 \varepsilon_0^2 / \alpha_0^2$ (i.e., a bound on the Lebesgue measure of

the state-space region where the HJI-VI is violated), which remains small relative to \mathcal{X} as demonstrated in Sec. V.

With the above formulation, when D_{violate} is active, we replace the gradient of the learned value function with the pre-computed offline substitute $\tilde{V}_\phi^\dagger(\mathbf{x}, t) = \max\{V_\phi^\dagger(\mathbf{x}, t), g(\mathbf{x})\}$ for a small time step, where V_ϕ^\dagger is the obstacle-free true value function satisfying the HJI-PDE. Thus, we guarantee that $\tilde{V}_\phi^\dagger(\mathbf{x}, t) \geq g(\mathbf{x})$ and $\mathbf{D}_t(\mathbf{x}, t) \leq 0$ for all $(\mathbf{x}, t) \in \mathcal{X} \times [0, T]$.

We now formalize a contingency control policy that guarantees finite-time reachability to \mathcal{L} . Let $\mathbf{u}_\phi^*(\mathbf{x}, t)$ and $\mathbf{u}_\mathcal{L}^*(\mathbf{x}, t)$ denote the optimal controls computed via (2) using $\nabla_{\mathbf{x}} \tilde{V}_\phi(\mathbf{x}, t)$ and $\nabla_{\mathbf{x}} \tilde{V}_\phi^\dagger(\mathbf{x}, t)$, respectively. The contingency switching policy is defined as

$$\mathbf{u}^*(\mathbf{x}, t) = \begin{cases} \mathbf{u}_\phi^*(\mathbf{x}, t), & (\mathbf{x}, t) \notin D_{\text{violate}}, \\ \mathbf{u}_\mathcal{L}^*(\mathbf{x}, t), & (\mathbf{x}, t) \in D_{\text{violate}}, \end{cases} \quad (9)$$

Outside D_{violate} , \tilde{V}_ϕ satisfies the HJI-VI descent condition, enforcing strict decrease toward \mathcal{L} along certified reach-avoid trajectories. Within D_{violate} , the fallback \tilde{V}_ϕ^\dagger acts as a control Lyapunov function admitting strict descent toward \mathcal{L} , which will drive the state out of the violation region. Thus, we apply $\mathbf{u}_\mathcal{L}^*$ until the trajectory exits D_{violate} in finite time, thereby guaranteeing that switching remains transient. Since $\mathcal{RA}_\phi^e(t) \subseteq \mathcal{RA}^\dagger(t)$, any state with $\tilde{V}_\phi(\mathbf{x}, t) \leq 0$ satisfies $g(\mathbf{x}) \leq 0$, ensuring the fallback control preserves forward invariance of \mathcal{L} and cannot drive the system into \mathcal{G} .

V. SIMULATION RESULTS

A. FNO Training and Implementation

A dataset of $|\mathcal{S}_{\text{train}}| = 100$ samples was generated, each with a fixed \mathcal{L} centered at the origin in $D^{\text{loc}} = [-10, 10]^2$ and a single randomly generated obstacle $(x_{\mathcal{O}}, y_{\mathcal{O}}) \in D^{\text{loc}}$, $r_{\mathcal{O}} \in [0.5, 2]$. Training on a single obstacle per sample suffices, as the operator generalizes to multiple obstacles by evaluating local spatial region independently. The training data is computed over $T = 8$ on a $[50, 50, 25, 33]$ grid in $[x, y, \theta, t]$, governed by (3) with $v \in [0, 1]$, $\omega \in [-1, 1]$, and $\mathbf{d} = [0.1, 0.1, 0.1]$. The FNO comprises $B = 4$ Fourier layers with lifting dimension $d_v = 64$, input channels $\{g(\mathbf{x}), x, y, \theta, t\}$ ($d_a = 5$), output $\{V_\phi\}$ ($d_y = 1$), and ReLU activations. Training ran for 3000 epochs with Adam, taking ≈ 9 hours on an Intel i7, 16 GB RAM, NVIDIA RTX 4050. During online inference, we leverage FNO zero-shot super-resolution to predict a reachable set over finer grid of size $[100, 100, 17, 17]$ for $[x, y, \theta, t]$. Since (θ, t) are hyperparameter, we limit the total number of query points.

1) *Evaluating universal approximation theorem for FNO*: We generated $|\mathcal{S}_{\text{test}}| = 100$ additional test data to evaluate the universal convergence of the HJI-VI solution operator in Assumption 2, with metrics summarized in Table I across 1500–3000 training epochs. Let $e = V_\phi - V^\dagger$.

Underapproximation guarantee. At each reported epoch, we provide the L^∞ upper bound $\varepsilon \geq \|e\|_\infty$ over $|\mathcal{S}_{\text{test}}|$ to validate the underapproximation guarantees in Lem. 1. First, we define the *inclusion volume*, i.e., the proportion of the learned reachable set lying inside the true reachable

set, evaluated over the \mathcal{X} -grid for all $t \in [0, T]$: $\eta_{\text{include}} := \text{Vol}(\mathcal{R}\mathcal{A}_\phi \cap \mathcal{R}\mathcal{A}^\dagger) / \text{Vol}(\mathcal{R}\mathcal{A}_\phi)$. We report η_{include} for both the ε - and 0-sublevel sets of the learned reachable set. Constraining to the ε -sublevel set achieves $\eta_{\text{include}} = 1$ across all training epochs, guaranteeing $\mathcal{R}\mathcal{A}_\phi^\varepsilon(t) \subset \mathcal{R}\mathcal{A}^\dagger(t)$ throughout the contingency maneuver. Additionally, the 0-sublevel set yields a close approximation as evidenced by the small mean squared error (MSE) in order of 10^{-4} . **Violation measure bound.** We evaluate the L^2 gradient error $\varepsilon_0 \geq \|\nabla_{\mathbf{x}} e\|_{L^2}$ to bound $\text{meas}(D_{\text{violate}})$ relative to \mathcal{X} , as discussed in Sec. IV-D.2. For our unicycle dynamics (3), $M_f = \sqrt{2}$. Our data shows uniformly that $\|\partial_t e\|_{L^2} \leq 0.404 M_f \|\nabla_{\mathbf{x}} e\|_{L^2}$. Assuming a descent margin $\alpha_0 = 0.03$, the normalized violation fraction satisfies $\text{meas}(D_{\text{violate}}) / \text{meas}(\mathcal{X}) \leq 1.404^2 M_f^2 \varepsilon_0^2 / (\alpha_0^2 \cdot 800\pi)$, where $\text{meas}(\mathcal{X}) = 800\pi$ for $\mathcal{X} \doteq D^{\text{loc}} \times \mathbb{S}^1$. After 3000 training epochs, the violation region occupies only $\approx 2.01\%$ of the state space, indicating that gradient inconsistencies are confined to a small volumetric subset rather than forming a connected separating manifold. The violation region is therefore measure-negligible, ensuring the switching contingency control law (9) is well-posed over \mathcal{X} at each time step.

B. Case studies

1) *Contingency planning case study:* We evaluate the contingency policy (9) for finite-time reachability toward \mathcal{L} within $T = 8$ across scenarios with 1–7 a priori unknown obstacles. The robot’s initial state is randomly generated such that it neither intersects any obstacle nor lies outside $\mathcal{R}\mathcal{A}_\phi^\varepsilon(t)$ for $t \in [4, 8]$. At each run, we first determine the minimum time $t_{\text{min}} \in [4, 8]$ such that the reachable set contains the robot’s state, i.e., $V_\phi(\mathbf{x}, t_{\text{min}}) \leq 0$, then apply control policy (9) under worst-case disturbance until \mathcal{L} is reached. Upon detection of an unknown obstacle, $V_\phi(\mathbf{x}, t)$ is updated, t_{min} is recomputed, and the total duration T_{reach} is accumulated. A run is marked as a failure if either $g(\mathbf{x}) > 0$ (obstacle collision) or $V_\phi(\mathbf{x}, 0) > 0$ (outside the reachable set at final time). Each scenario is repeated over 500 runs, with metrics including success rate, average T_{reach} , and for failures, the average value function at final time and distance to \mathcal{L} , summarized in Table II.

Overall, the policy achieves a success rate above 95.6% across all unknown obstacle configurations under worst-case disturbance. Stronger guarantees is shown for the single-obstacle case where V_ϕ updates less frequently. All failures are attributed solely to $V_\phi(\mathbf{x}, 0) > 0$; frequent obstacle configuration changes cause the policy in (9) to act optimally at current time step but may yield suboptimal trajectories over

TABLE I: FNO Training and Approximation Metrics

Training Epochs	ε (L^∞)	η_{include} ($\mathcal{R}\mathcal{A}_\phi^\varepsilon / \mathcal{R}\mathcal{A}_\phi$)	ε_0 ($\mathbb{W}^{1,2}$)	$\text{meas}(D_{\text{violate}})$ over $\text{meas}(\mathcal{X})$	MSE [$\times 10^{-4}$]
1500	0.483	1.0 / 0.9927	0.118	2.465 %	9.62
2000	0.455	1.0 / 0.9928	0.114	2.281 %	8.60
2500	0.442	1.0 / 0.9937	0.110	2.138 %	7.84
3000	0.431	1.0 / 0.9935	0.107	2.011 %	7.06

subsequent steps due to unpredictable obstacles. Nonetheless, by conditioning on the reachable set as in Sec. IV-D.1, $g(\mathbf{x}) \leq 0$ always holds and no obstacle collision occurs. Additionally, failure cases remain close to the reachable set boundary, with $|V_\phi(\mathbf{x}, 0)| \leq 0.111$ and small average distance to \mathcal{L} at final time.

2) *Multi-goals Planning Framework Case Study:* We evaluate our framework for $K = 6$ goals over $\Omega = [-25, 25]^2$, with each RRT^X tree initialized with $n_{\mathcal{V}} = |\mathcal{V}| = 2,000$ nodes. The goal set $\mathbf{P}_{\text{goals}}$ is fixed and hand-selected to ensure feasibility, with the robot’s initial position coinciding with a randomly selected goal per trial. We consider two extreme cases: a fully *unknown* and an *a priori* known obstacle map, the latter serving as a baseline for asymptotically optimal convergence of our planner. Additionally, the framework is evaluated with and without the reachability-based constraints in Sec. IV-C.2. Performance is measured by total traversed distance (Dist.) and execution time (Time), and the results are averaged over 10 trials and reported in Table III. Sample runs are shown in Fig. 3.

Under unknown obstacles, trajectory costs remain comparable to the known-map baseline, which demonstrates that locally optimal goal sequencing remains effective in large-scale environments. The increased execution time arises from RRT^X rewiring cascades upon obstacle discovery. Imposing reachability constraint empirically increases execution time, as nodes sampled near the boundary of Ω_{feasible} are frequently rejected during tree expansion—a limitation similarly identified in [15], which is mitigated by eliminating Voronoi bias in the sampling strategy. Nonetheless, the constrained planner converges to a minimum-cost path and goals sequence with comparable distances to unconstrained cases.

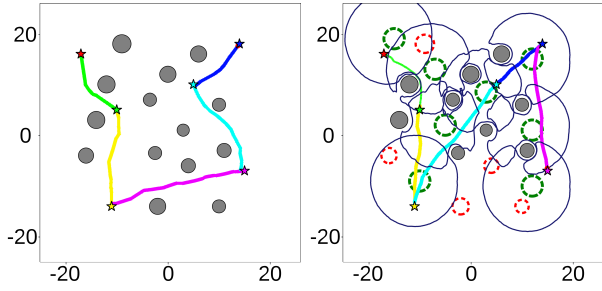
3) *KUKA’s youBot simulation:* We tested our framework in real-time on KUKA’s youBot in Webots simulation as seen in footnote 1 and shown in Fig. 4. The environment is of size $\Omega = [-10\text{m}, 10\text{m}]^2$ and the youBot is equipped with LIDAR sensor with range $r_{\text{sense}} = 5.5\text{m}$. When wooden crates (obstacles) enter the sensing range of the robot, the robot detects their boundaries and constructs circular over-approximations, which demonstrates the generalizability of our FNO model trained with circular obstacle representations. When follow-

TABLE II: Contingency Policy Case Studies (500 runs each)

Scenario	Success	Avg. T_{reach}	Avg. $V(\mathbf{x}, 0)$ (failure)	Avg. Dist. to \mathcal{L} (failure)
1 Obs	100%	4.564	—	—
3 Obs	98.00%	4.600	0.054	1.544
5 Obs	96.80%	4.769	0.111	1.582
7 Obs	95.60%	4.707	0.019	2.046

TABLE III: Multi-Goals Planning Case Studies (10 runs each)

RRT ^X Constraint	Unknown Map		Priori-Known Map	
	Dist.	Time	Dist.	Time
$\mathbf{p} \in \Omega_{\text{feasible}}$	105.614	89.494s	105.428	64.741s
$\mathbf{p} \in \Omega$	103.879	47.604s	102.568	42.067s



(a) Known map & no reachability (b) Unknown map & reachability

Fig. 3: Comparison of two cases in the multi-goal planning and routing framework: (a) an environment with known obstacles (grey) and no reachable-set constraint for contingency planning; (b) an environment in which all obstacles are a priori unknown (red, dashed) and later detected (grey), with a guaranteed finite-time reachability strategy to a safe set (green, dashed) enforced at every state along the trajectory. The robot starts at the red star, and trajectory colors denotes the sequence of the goals visited.

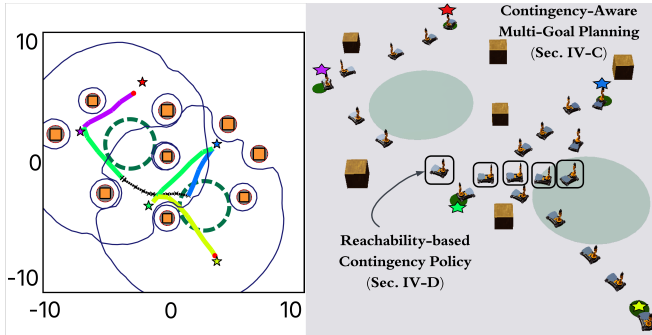


Fig. 4: Contingency-aware multi-goal planning on KUKA's youBot simulation. On the plot, the robot initializes at the red star, and the trajectory color encodes the active goal index. While navigating toward the green star, an adversarial event is triggered and activates the contingency mechanism, prompting the robot to execute a certified fallback policy (black, squared) toward the safe set (green, dashed). Upon reaching the safe set, the robot resumes the mission and visits the remaining goals in a locally optimal sequences.

ing RRT^X path, we apply two-phase control strategy: in-place turning $\mathbf{u}_p = (0, \omega_p)$ and forward translation $\mathbf{u}_p = (v_p, 0)$. During execution, adversarial events are randomly triggered to activate the contingency controller (9), at which point the robot switches to the certified gradient-based feedback law. Linear and angular velocity commands are mapped to individual wheel velocities. Despite multiple contingency activations (e.g., during the initial approach to the green goal), the robot safely recovers and completes all remaining goals under a locally optimal sequencing policy.

Time complexity. RRT^X costs $\mathcal{O}(n_V \log n_V)$ and Held-Karp solves with $\mathcal{O}(K^2 \cdot 2^K)$. In a dynamic environment with H obstacles, each update may trigger a full replanning cycle, raising the worst-case total to $\mathcal{O}(H \cdot K^2 \cdot 2^K \cdot n_V \log n_V)$. Nonetheless, 2^K term remains as the dominant bottleneck. Thus, our algorithm is viable in real-time for $K \leq 8$.

VI. CONCLUSION

In this work, we develop a solution operator learning framework for Hamilton–Jacobi reach–avoid differential game using a Fourier Neural Operator and establish a provably safe under-approximation of the true backward reachable set through universal approximation theorem. We further certify the associated control policy and guarantee finite-time reachability to a designated safe set under worst-case disturbances. We integrate the certified reachable set into an online, contingency-aware multi-goal planning framework that achieves asymptotically optimal routing while ensuring disturbance-robust safety and state-wise feasibility of a recovery strategy in unknown environments.

REFERENCES

- [1] E. C. Kerrigan, “Predictive control for linear and hybrid systems [bookshelf],” *IEEE Control Systems Magazine*, vol. 38, no. 2, pp. 94–96, 2018.
- [2] A. D. Ames, X. Xu, J. W. Grizzle, and P. Tabuada, “Control barrier function based quadratic programs for safety critical systems,” *IEEE Trans. on Automatic Control*, vol. 62, no. 8, pp. 3861–3876, 2017.
- [3] Y. Chen, M. Jankovic, M. Santillo, and A. D. Ames, “Backup control barrier functions: Formulation and comparative study,” in *60th IEEE Conf. on Decision and Control (CDC)*. IEEE, 2021, pp. 6835–6841.
- [4] K. Margellos and J. Lygeros, “Hamilton–jacobi formulation for reach–avoid differential games,” *IEEE Transactions on Automatic Control*, vol. 56, no. 8, pp. 1849–1861, 2011.
- [5] S. Bansal and C. J. Tomlin, “Deepreach: A deep learning approach to high-dimensional reachability,” in *2021 IEEE International Conference on Robotics and Automation (ICRA)*, 2021, pp. 1817–1824.
- [6] A. Singh, Z. Feng, and S. Bansal, “Exact imposition of safety boundary conditions in neural reachable tubes,” in *Proceedings of the IEEE International Conference on Robotics and Automation (ICRA)*, 2025.
- [7] M. Tayal, A. Singh, S. Kolathaya, and S. Bansal, “A physics-informed machine learning framework for safe and optimal control of autonomous systems,” 2025. [Online]. Available: <https://arxiv.org/abs/2502.11057>
- [8] J. Borquez, K. Nakamura, and S. Bansal, “Parameter-conditioned reachable sets for updating safety assurances online,” in *IEEE International Conf. on Robotics and Automation (ICRA)*, 2023, pp. 10 553–10 559.
- [9] K.-C. Hsu, V. Rubies-Royo, C. J. Tomlin, and J. F. Fisac, “Safety and liveness guarantees through reach-avoid reinforcement learning,” in *Proc. of Robotics: Science and Systems (RSS)*, vol. XVII, 2021.
- [10] V. Rubies-Royo, D. Fridovich-Keil, S. Herbert, and C. J. Tomlin, “A classification-based approach for approximate reachability,” in *International Conf. on Robotics and Automation (ICRA)*, 2019, pp. 7697–7704.
- [11] Y. Li and M. Chen, “Hjmo: Hamilton-jacobi reachability with neural operators,” 2025. [Online]. Available: <https://arxiv.org/abs/2504.19989>
- [12] D. S. Johnson and L. A. McGeoch, “The traveling salesman problem: A case study in local optimization,” 2008. [Online]. Available: <https://api.semanticscholar.org/CorpusID:208903251>
- [13] D. Perez, P. Rohlfshagen, and S. M. Lucas, “The physical travelling salesman problem: Wcci 2012 competition,” in *2012 IEEE Congress on Evolutionary Computation*, 2012, pp. 1–8.
- [14] S. Karaman and E. Frazzoli, “Sampling-based algorithms for optimal motion planning,” *The International Journal of Robotics Research*, vol. 30, no. 7, pp. 846–894, 2011. [Online]. Available: <https://doi.org/10.1177/0278364911406761>
- [15] J. Janoš, V. Vonásek, and R. Pěnička, “Multi-goal path planning using multiple random trees,” *IEEE Robotics and Automation Letters*, vol. 6, no. 2, pp. 4201–4208, 2021.
- [16] B. Englot and F. S. Hover, “Three-dimensional coverage planning for an underwater inspection robot,” *The International Journal of Robotics Research*, vol. 32, no. 9-10, pp. 1048–1073, 2013. [Online]. Available: <https://doi.org/10.1177/0278364913490046>
- [17] S. Bansal, M. Chen, S. Herbert, and C. J. Tomlin, “Hamilton-jacobi reachability: A brief overview and recent advances,” in *56th IEEE Conf. on Decision and Control (CDC)*, 2017, pp. 2242–2253.

- [18] Z. Li, N. Kovachki, K. Azizzadenesheli, B. Liu, K. Bhattacharya, A. Stuart, and A. Anandkumar, "Neural operator: Graph kernel network for partial differential equations," 2020. [Online]. Available: <https://arxiv.org/abs/2003.03485>
- [19] N. Kovachki, S. Lanthaler, and S. Mishra, "On universal approximation and error bounds for fourier neural operators," *Journal of Machine Learning Research*, vol. 22, pp. 1–76, 2021. [Online]. Available: <https://dl.acm.org/doi/10.5555/3546258.3546548>
- [20] S. Lanthaler, Z. Li, and A. M. Stuart, "Nonlocality and nonlinearity implies universality in operator learning," *Constructive Approximation*, vol. 62, pp. 261–303, 2025.
- [21] I. M. Mitchell, "A Toolbox of Level Set Methods," Department of Computer Science, University of British Columbia, Tech. Rep. TR-2007-11, 2007, version 1.1.1, accessed 15 Feb 2026. [Online]. Available: <https://www.cs.ubc.ca/~mitchell/ToolboxLS/>
- [22] L. C. Evans, "Measure theory and fine properties of functions," 1992. [Online]. Available: <https://api.semanticscholar.org/CorpusID:118983299>
- [23] M. Otte and E. Frazzoli, "Rrtx: Asymptotically optimal single-query sampling-based motion planning with quick replanning," *The International Journal of Robotics Research*, vol. 35, no. 7, pp. 797–822, 2016. [Online]. Available: <https://doi.org/10.1177/0278364915594679>
- [24] M. Held and R. M. Karp, "A dynamic programming approach to sequencing problems," *Journal of the Society for Industrial and Applied Mathematics*, vol. 10, no. 1, pp. 196–210, 1962. [Online]. Available: <https://doi.org/10.1137/0110015>
- [25] G. B. Folland, *Real Analysis: Modern Techniques and Their Applications*, 2nd ed. John Wiley & Sons, 2013.